Journal of Saudi Chemical Society (2018) **22**, 937–948

King Saud University

Journal of Saudi Chemical Society

www.ksu.edu.sa
www.sciencedirect.com

ORIGINAL ARTICLE

Degradation of Methyl Parathion, a common pesticide and fluorescence quenching of Rhodamine B, a carcinogen using β-D glucan stabilized gold nanoparticles

Sutanuka Pattanayak [a], **Sharmila Chakraborty** [b], **Suman Biswas** [a], **Dipankar Chattopadhyay** [c], **Mukut Chakraborty** [a,*]

[a] *Department of Chemistry, West Bengal State University, Barasat, Kolkata 700126, West Bengal, India*
[b] *Department of Microbiology, Sammilani Mahavidyalaya, Baghajatin, E.M. Bypass, Santoshpur, Kolkata 700094, West Bengal, India*
[c] *Department of Polymer Science & Technology, University of Calcutta, 92, A.P.C. Road, Kolkata 700009, West Bengal, India*

Received 15 November 2017; revised 13 February 2018; accepted 15 February 2018
Available online 23 February 2018

KEYWORDS

β-D-Glucan;
Gold nanoparticles;
Green synthesis;
Methyl Parathion;
Fluorescence quencher

Abstract Natural carbohydrate polymer β-D-glucan extracted from *Tricholoma crassum* (Berk.) Sacc. predominantly linked by β-glycosidic bonds have been used to synthesize gold nanoparticles (Au NPs). As glucan is water soluble, the Au NPs are prepared in water medium, a green solvent. The morphology and characterization of the synthesized Au NPs have been confirmed by various techniques, like TEM, EDX, XRD, UV–Vis and FT-IR spectroscopic studies. The obtained Au NPs exhibits chemosensing property against Methyl Parathion, a group of highly toxic organophosphorous pesticide, extensively used as an agricultural chemical. Degradation of parathion using Au NPs lead to water-soluble products thereby reducing the toxicity of Methyl Parathion by disrupting the thiophosphate-ester linkage. The synthesized Au NPs also act as a good fluorescence quencher of Rhodamine B, a common fluorophore and carcinogenic compound, obeying Stern-Volmer equations. The β-D-glucan capped Au NPs are safe having possible medicinal usage.

1. Introduction

Physico-chemical properties of metal nanoparticles have been extensively studied, leading to their use in different fields like catalysis, optics, electronics, and biotechnology [1–5]. Noble metal nanoparticles like Silver and Gold have proved their versatility in application areas such as catalysis [6,7], biological sensing and imaging [8], optics [9], chemical sensor [10],

* Corresponding author.
E-mail address: mukutchem@yahoo.co.in (M. Chakraborty).
Peer review under responsibility of King Saud University.

Production and hosting by Elsevier

https://doi.org/10.1016/j.jscs.2018.02.004
1319-6103

antimicrobial and anticancer activity [11,12] and in various other fields [13].

The frequently used synthesis routes for metal nanoparticles make use of chemical reducing agents like sodium borohydride, N,N-dimethylformamide, trisodium citrate and other organic compounds [5,14,15]. Potential environmental risk associated with chemical toxicity and bio-hazard is becoming the main opposing factors against the rampant use of chemical reducing agents. Over the past few years, targeting the fundamental principles of green chemistry, scores of attempts have been made to synthesize nanoparticles using green techniques [16,17]. Different precursors, like biomolecules and bioorganisms [18,19], peptides [20,21], plant extracts [22,23] and biopolymers [24] have been used for the synthesis of nanoparticles, mostly for their environment friendly attribute. Polysaccharides, an essential natural resource have also been used along with various biological materials, for the synthesis of metal nanoparticles. Raveendran et al., 2003 reported the preparation of silver nanoparticles using β-D-glucose as a reducing agent and starch as capping agent [25]. Mukherjee et al., 2001 reported a novel biological method for the synthesis of gold nanoparticles using the fungus Verticillium [26]. Biosynthesis of Au, Ag and Au-Ag nanoparticles using edible mushroom extract was reported by Philip [27].

β-D-Glucans originate from bacteria, algae, yeasts, mushrooms, moulds and higher plants, and consequently, their structure depends on the source from which they were isolated [28–30]. Fungal β-glucans provide a major health benefit to humans as they bind to membrane receptor and exhibit anticancer, immune-modulating, anti-cholesterolemic, hepatoprotective and neuroprotective activities [31–33]. β-D-Glucan isolated from *Ganoderma lucidum* (Fr.) Karst, a mushroom, is used as a traditional medicines in many Asian countries. These fungal polysaccharides are especially used as a rich protein source and in the development of biomedical drugs. However, mixed solubility reports of β-glucans in aqueous medium is a major obstacle to its clinical utilization. Specifically, (1 → 3)-β-glucan exists as an insoluble microparticulate in aqueous medium upon initial isolation from *G. Lucidum*, and topical administration of insoluble microparticulates of (1 → 3)-β-glucan induces no toxicity. However, Williams et al. have demonstrated that (1 → 3)-β-glucan isolated from yeast, *Saccharomyces cerevisiae* is water-soluble and immunologically active [34,35]. *Tricholoma crassum* (Berk.) Sacc., family Tricholomataceae [36] is an ectomycorrhizal fungus [37,38] which is edible and non-toxic [38,39]. The nutritional value of *T. crassum* is very promising [40] and the method of cultivation of this mushroom has been commercially exploited. Synthesis of silver nanoparticles [41] with the extract of mycelium of *T. Crassum* (Berk.) Sacc. and the fibrinolytic activity [42] using fruit bodies are also reported. Recently, the detailed structural characterization of the heteropolysaccharide and its immunological activity from the alkaline extract of *T. crassum* (Berk.) Sacc were carried out and reported [43]. The major bioactive polysaccharides isolated from *T. crassum* (Berk.) Sacc. are β-(1 → 3) and β-(1 → 6)-D-glucans. Detailed work related to the structural characterization, immunological, and lipid peroxidation properties of the polysaccharide isolated from the aqueous extract of the fruit bodies of *Tricholoma crassum* (Berk.) Sacc. have also been reported [44].

We report here the synthesis of gold nanoparticles (Au NPs) with the crude form of the extracted β-D-glucans from bodies of ectomycorrhizal edible mushroom *Tricholoma crassum* (Berk.) Sacc. The Au NPs synthesized are of different shape and we have been able to prepare multi-pod gold nanostructures with this polysaccharide. The Au NPs have been studied using various spectroscopic and characterization techniques. Diffraction studies have been done to confirm nanoparticle formation. The synthesized Au NPs exhibit Chemosensor activity. Hence these glucan stabilized Au NPs have been used as colorimetric sensor for detection and estimation of pesticide present in the environment in aqueous medium. We have also schematically proposed the mechanism of degradation of the pesticide, Methyl Parathion in presence of the nanoparticles.

These nanostructures are also able to quench the strong fluorescence of dyes like Rhodamine B. The β-D-Glucan capped Au NPs are non-toxic and can have possible medicinal applications.

Au NPs find various biomedical applications and knowledge about their toxicity and health impacts helps us to use these in real clinical settings. Nanomaterials, if toxic for environmental bacteria, have devastating effect on the ecosystems and leads to ecological imbalance. Alternately, if the bacteria are resistant to nanomaterials, they can be used to adsorb them onto their membrane or cells so they can be responsible for their transfer in the environment. This leads to the transfer of NPs from contaminated to non-contaminated areas. Hence, the antimicrobial and toxicity studies of the glucan stabilized Au NPs were also carried out.

2. Experimental

2.1. Materials

β-D-Glucan extracted from *Tricholoma crassum* (Berk.) Sacc., Tetra-chloroauric (III) acid ($HAuCl_4$, Sigma–Aldrich, Steinheim, Germany) solution of 10^{-2} M concentration, Nutrient agar from Hi Media and triple distilled water were used to synthesize the Au NPs. Mouse fibroblast (L929) cell lines were purchased from National Centre for Cell Science, Pune, India. Cell culture media and all the other materials required for culturing were obtained from Gibco, USA.

2.2. Synthesis of gold nanoparticles

A 0.05% aqueous solution of β-D-glucan was prepared by continuous stirring on a magnetic top at room-temperature. The prepared glucan solution was then placed on a water bath maintained at 70–80 °C and to the hot glucan solution 10^{-2} M auric chloride solution was added drop wise under stirring condition. A dark violet coloured solution was obtained after about 30 min indicating the formation of Au NPs. The Au NPs were preserved for subsequent characterization.

2.3. Characterization of gold nanoparticles

2.3.1. Uv–visible spectral analysis

The obtained dark violet coloured solution was characterized using UV–Vis spectrophotometry. The spectra were recorded on a double beam spectrophotometer (Perkin Elmer Lambda 25) from 200 to 800 nm at a resolution of 1 nm. The UV–Vis

spectra of 0.05% β-glucan solution and glucan stabilized Au NP was recorded using triple distilled water as reference. Formation of Au NPs was indicated by the appearance of the typical SPR band characteristic of Au NPs in the UV–Vis spectra.

2.3.2. High resolution-transmission electron microscopy (HR-TEM) and energy dispersive X-ray (EDX) analysis

The size and shape of the synthesized gold nanoparticles were subsequently studied using a High Resolution Transmission Electron Microscopy (HRTEM) equipped with energy dispersive X-ray (EDX) spectrometer. The sample was prepared by casting a drop of the diluted and ultra-sonicated Au NPs solution on a 300 mesh carbon coated copper grid and air-dried. HRTEM images were taken on JEOL JEM 2100 equipped with a Gatan Image Filter operated at an accelerating voltage of 200 kV.

The HRTEM instrument was also equipped with Energy dispersive X-ray (EDX) technology. The EDX spectrum of the sample was measured with the same carbon coated copper grid and helps in confirming the formation of gold nanoparticles.

2.3.3. Fourier transform-infrared (FT-IR) spectra analysis

To obtain dried, solid Au NPs the solution was centrifuged at 10,000 rpm speed for 20 min. The concentrated solution was washed 4–5 times with triple distilled water to remove excess glucan adsorbed on the particles. Thereafter, the supernatant solution was decanted leaving the black precipitate which was collected and dried for further use. The purified powder of Au NPs was subjected to Fourier Transform-Infrared (FT-IR) spectroscopic measurement. These measurements were carried out on a Perkin Elmer spectrum two instrument in the diffuse reflectance mode at a resolution of 4 cm^{-1} in KBr pellets. For comparison, finely powdered glucan was mixed with KBr powder and pelletized which were also subjected to similar spectroscopic measurement. In case of liquid samples, the Attenuated Total Reflectance (ATR) attachment with ZnSe crystal was used.

2.3.4. X-ray diffraction (XRD) analysis

The crystalline pattern of the synthesized Au NPs were confirmed by X-ray Diffraction (XRD) technique. Using step scan technique XRD was studied using a PANalytical: XPERT-PRO equipment with pure CuKα radiation produced from a Johansson monochromator. The sample was prepared on a glass slide using the centrifuged solution of Au NPs, which was scanned from 10 to 120° (2θ) after drying.

2.4. Chemosensor application of glucan capped Au NPs by breaking organophosphate ester

The glucan capped Au NPs were mixed with Methyl Parathion (MP), a common pesticide to understand the interactions between the substrates. A coarse water solution of MP was prepared by adding ~2 μL of it into 10 ml of distilled water which was labelled as set 1. Set 2 contained the same methyl parathion stock solution along with glucan capped Au NPs solution. The pH of these solutions was tested with a pH meter and was about 7 and 5 for set 1 and 2, respectively. Subsequently, set 3 was prepared by adding a very small amount of NaOH solution into MP-Au NPs solution such that the pH of the solution was about 9. The different sets were studied as given below.

2.4.1. UV–Vis spectrophotometric and FT-IR spectrophotometric observations

The different sets prepared above were allowed to homogenize and were scanned using a UV–Vis spectrophotometer in the range 200–800 nm using triple distilled water as reference.

The data obtained from UV–Vis spectroscopy was subsequently checked and correlated through FT-IR spectroscopy. Here, we have used the Attenuated Total Reflectance (ATR) mode to scan the liquid samples in the range 4000–400 cm^{-1} where the ZnSe crystal was loaded with the solution one by one.

2.5. Fluorescence quenching of synthesized Au NPs

Being electron rich moiety, Au NPs are capable of quenching the fluorescence intensity of any fluorescent probe as the nanoparticles remain surrounded by a strong Plasmon field [45]. To investigate the quenching property of Au NPs, the glucan capped Au NPs were mixed with a well known fluorescent probe Rhodamine B. Rhodamine B exhibits multiple peaks having maximum absorbance at 360 nm, with well defined peak sharpness. This lead us to use an excitation wavelength of 360 nm for fluorometric experiments. The emission spectra were recorded in the range of 370–700 nm. The fluorescence spectra exhibited a maximum intensity at 578 nm and the subsequent quenching studies were carried out at that wavelength. A total volume of 100 μL of Glucan capped Au NPs solution in portions of 10 μL each were added to the Rhodamine B solution (10^{-6} M) and the spectra recorded after each addition. We know that the Stern-Volmer constant (K_{sv}) value depends upon the temperature [46] as well as the viscosity of the medium The quenching studies were carried out in four solvents viz., Water (0.89 cP), Ethanol (1.095 cP) Isopropanol (1.96 cP) and Ethylene glycol (16.10 cP) having different viscosities keeping the temperature constant at 25 °C. The fluorescent probe Rhodamine B was prepared in these four solvents separately and quenching study was done as described.

2.6. Antimicrobial and antitoxicity study of synthesized Au NPs

The antimicrobial activity of glucan stabilized Au NPs was studied on Gram positive bacteria *Staphylococcus aureus* and Gram negative bacteria *Klebsiella aerogenes* and *Escherichia coli* using standard protocol [47]. Following overnight incubation, the diameter of zones of inhibition were measured and recorded. A minimum of at least three readings were taken for reporting.

The growth curves at room temperature of the Au NPs were studied to understand their antitoxicity effect. *Escherichia coli* (*E. coli*) cells were grown overnight in presence of glucan stabilized Au NPs and the supernatant obtained during nanoparticle synthesis for experimental study. Similar cells were grown in nutrient broth as control. For the purpose of experiment, 100 μL of supernatant and 100 μL of Au NPs were added to 25 ml of bacterial culture and grown for 15–16 h. The following day 4.5 ml of overnight culture of each type was added to fresh nutrient broth and the volume made up to

50 ml. The bacterial growth (indicated by change in absorbance values) in presence and absence of Au NPs were taken at intervals of 30 min at 600 nm using a UV–Vis spectrophotometer.

L929 (1×10^5 cells/mL) cells were plated in 96-well microtiter plates and incubated over- night for cell attachment. The medium was then removed and fresh medium, along with the corresponding sample concentrations (100–1000 μg/mL) were added to the cultures. Following treatment for 48 h at 37 °C, MTT solution (5 mg/mL in PBS) was added and incubation was prolonged for 4 h at 37 °C. Inhibition of cell proliferation was monitored by MTT (Himedia) assay [47]. Absorbance of the MTT-formazan product dissolved in DMSO (Himedia) was estimated at 595 nm using an ELISA plate reader (Thermo, USA).

3. Results and discussion

3.1. Polysaccharide characterization

The polysaccharide used in our study as reported earlier was white in colour and soluble in water having α-glucan and β-glucan content of 8.373 ± 3.148 g and 15.334 ± 1.183 g/100 g of polysaccharide, respectively. The β-(1-6)-glycosidic bonds exist in an ordered three-dimensional triple helical conformation as determined by Congo red studies [48].

3.2. Characterizations of glucan capped gold nanoparticles (Au NPs)

3.2.1. Uv–visible spectral analysis

The yellow coloured solution of β-D-glucan changed to a dark violet colour on addition of auric chloride and was studied using Ultraviolet–Visible spectrophotometry. The spectra of the resultant solution (Fig. 1, spectrum a) showed a sharp peak at 541 nm along with a broad hump at around 700 nm. The peak at 541 nm is characteristic of the SPR band of Au NPs and preliminary confirmed the formation of gold nanoparticles. The hump at higher wavelength may be due to the formation of some larger particles or particles of different shapes [49]. Fig. 1, spectrum 'b' represents the absorbance band of the β-D-glucan. In spectra 'b' there is only a small hump at ~255 nm which is slightly shifted to ~264 nm in spectra 'a'.

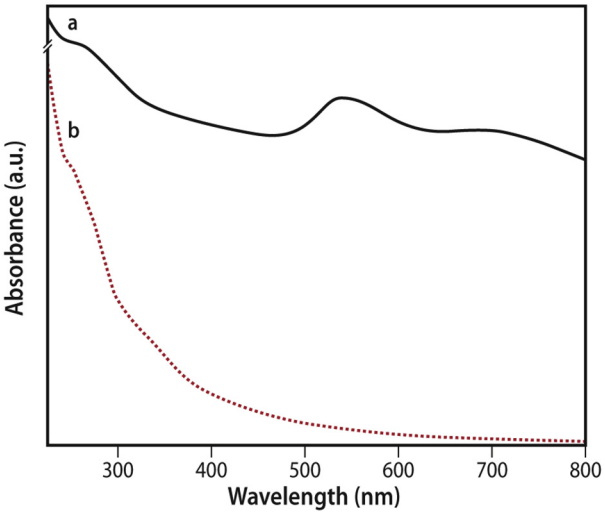

Fig. 1 (a) UV–vis spectra of glucan stabilized Au NPs and (b) β-glucan itself. The peak at around 541 nm corresponds to the surface plasmon resonance of Au NPs and double hump signifies the multi-structured Au NPs.

The slight shift in the peak position of glucan is probably due to involvement of the functional groups present in the biopolymer which act as binding sites for the Au NPs. However, the formation of the SPR peak at 541 nm which appears for Au NPs clearly confirms the formation of Au NPs.

3.2.2. High resolution-transmission electron microscopy (HRTEM) and energy dispersive X-ray (EDX) analysis

High resolution transmission electron microscopic (HRTEM) technique was employed to study the morphology of the synthesized nanoparticles. Fig. 2a-d depicted the images of the particles under an accelerating voltage of 200 kV. Starting from Fig. 2a to d the magnification of the micrographs was increased gradually. Fig. 2a clearly shows that particles of various shapes and sizes were generated which justify the appearance of double humped UV–Vis spectra which is normally observed when particles of different aspect ratio are synthesized [12]. Magnification was slightly increased in Fig. 2b and we observe that the particles which seemed to be spherical in Fig. 2a, are actually hexagons, pentagons etc. In Fig. 2c as we further increased the magnification, under higher resolution it was observed that the synthesized particles had pod like structures. This shows that the synthesized gold nanoparticles have multipod structures as we can clearly see different structures like hexagons, pentagons and rod shaped particles. Fig. 2d depicts the HRTEM image where the lattice fringes of the particle are clearly observed and the distance between them can be easily measured to ascertain the type of lattice formation.

The energy dispersive X-ray analysis (EDX) shown in Fig. 2e revealed strong signal of gold and again confirmed the formation of Au NPs. Metallic gold nanocrystals generally show typical optical absorption peak approximately at 2.983 keV due to surface Plasmon resonance. Peaks of carbon and copper were also obtained due to the carbon coated copper grid.

3.2.3. Fourier transform-infrared (FT-IR) spectra analysis

FT-IR analysis was done to identify the role of glucan in nanoparticles synthesis and stabilization. In the FT-IR spectrum of glucan (Fig. 3a), a broad stretching peak displayed around 3392 cm^{-1} is characteristic for hydroxyl group and the weak band at 2928 cm^{-1} is associated with the aliphatic C—H stretching vibration. The peaks at 1404 and 1078 cm^{-1} are possibly due to the bending vibrations of C—OH and the antisymmetric stretching band of C—O—C groups of polysaccharides [50]. In the FT-IR spectrum of Au NPs-glucan bioconjugates (Fig. 3b), a notch was observed in the region 1720–1740 cm^{-1}. To get a clear view, the region between 1700 and 1740 cm^{-1} is expanded and shown in higher resolution which clearly shows the presence of two small peaks at 1713 and 1730 cm^{-1}. Since a neutral polysaccharide (glucan) was used for the synthesis of Au NPs, peaks in the region of 1720–1740 cm^{-1} would not be usually expected but the appearance of two peaks (1713 and 1730 cm^{-1}) suggests that there

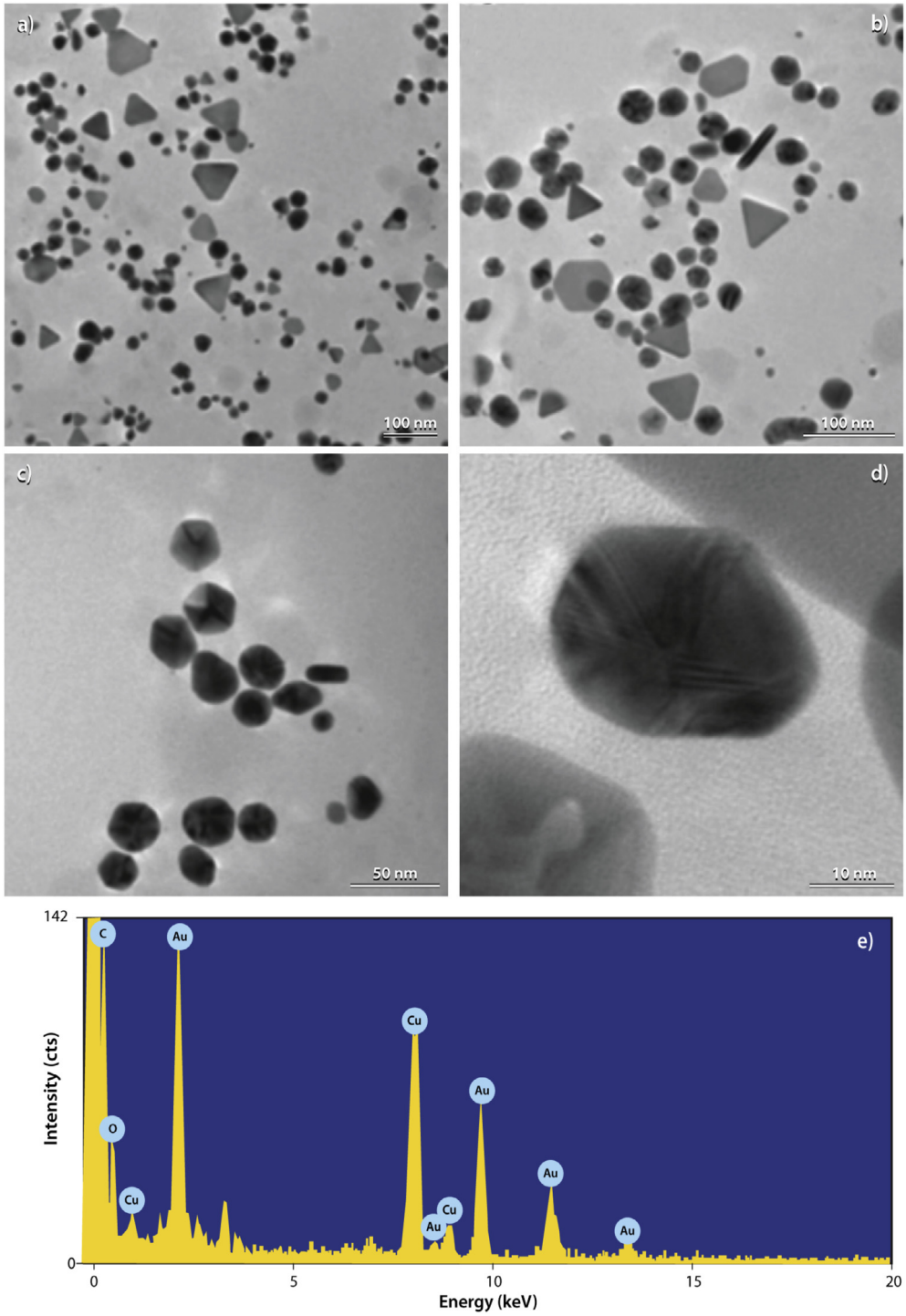

Fig. 2 (a) & (b) TEM images of multi-structured Au NPs, (c) Pod structured Au NPs are formed, (d) HRTEM image of Glucan capped Au NPs and (e) Energy dispersive X-ray (EDX) image of synthesized Au NPs.

must be some changes in the functionalities of glucan during the course of the reaction. The peaks at 1713 and 1730 cm^{-1} are probably due to the stretching vibrations associated with COOH group [51]. In acidic solution of $HAuCl_4$, there would be a possibility for cleavage of some glycosidic (C—O—C) linkages of the glucan chain and this may lead to the formation of some shorter segments with open chain structure [52]. In this open chain form there would be existence of potential CHO groups. Since, Au^{3+} ions are present in the reaction medium; these CHO groups would be readily oxidized to COOH groups with concomitant reduction of Au^{3+} to Au^0 [53]. Similar results have been observed in case of the glucan stabilized Au NPs. The slight shift in the peak positions is due to the interactions of the different groups of glucan with the Au NPs [47].

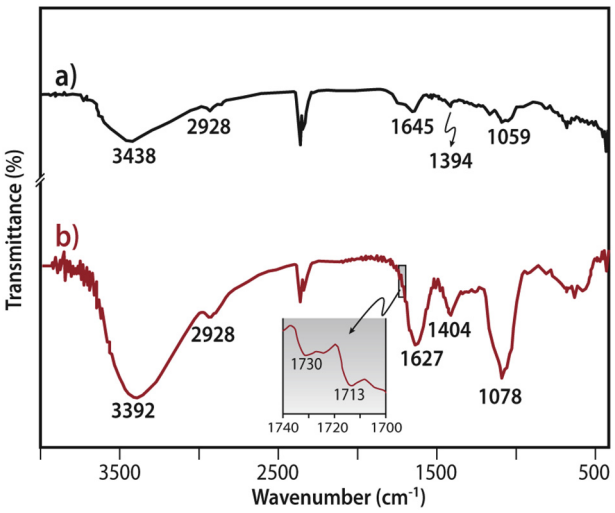

Fig. 3 FT-IR spectra of (a) 0.05% (w/v) glucan solution and (b) Au NPs-glucan bioconjugates prepared with 0.05% (w/v) glucan and 10^{-2} M $HAuCl_4$.

3.2.4. X-ray diffraction (XRD) analysis

X-ray diffraction (XRD) analysis further confirmed the crystalline nature of Au NPs. Fig. 4 shows the XRD patterns of Au NPs-glucan bioconjugates prepared with 10^{-2} M $HAuCl_4$. Diffraction peaks were obtained for 2θ values of 28.20, 38.21, 44.39, 64.76, 77.76, 81.72 and 115.20° and can be correlated to the (2 2 0), (1 1 1), (2 0 0), (2 2 0), (3 1 1), (2 2 2) and (4 2 0) planes respectively of face-centered cubic (fcc) lattice of Au NPs. The observed higher relative intensity of (1 1 1) diffraction peaks for the Au NPs prepared with the above mentioned concentrations of $HAuCl_4$ and of glucan (0.05%), presumably indicates greater exposure of the (1 1 1) facets to the crystal surface of Au NPs [54]. The lattice constant obtained for the (1 1 1) diffraction pattern was 4.066 Å for the Au NPs prepared for the mentioned concentration of $HAuCl_4$. The observed value was in close agreement with previous literature report (a = 4.0786 Å; Joint Committee on Powder Diffraction Standards file No. 04-0784).

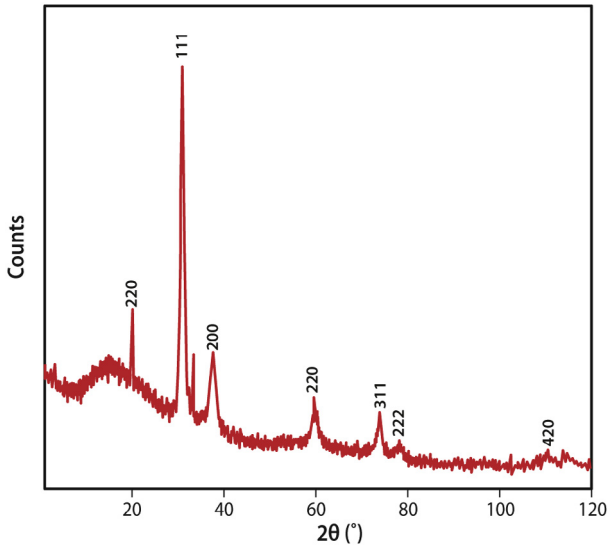

Fig. 4 XRD patterns of dried Au NPs-glucan bioconjugates prepared with 0.05% (w/v) glucan and 10^{-2} M $HAuCl_4$. Peaks could be indexed to FCC gold.

3.3. Cleavage of phosphate-ester bond of Methyl Parathion by glucan capped Au NPs

Methyl Parathion (MP), a very common pesticide renowned for its highly neurotoxic agricultural chemical property is extensively used world-wide to manage a wide range of insect pests. The environment including human health faces a deadly risk as its residue remains in the soil causing severe pollution. We have studied the sensing properties of glucan stabilized Au NPs towards methyl parathion by examining the UV–Vis spectral changes and its subsequent degradation at the ppm level.

3.3.1. UV–Vis spectrophotometric and FT-IR spectroscopic observations

Fig. 5a shows the UV–Vis spectrum of an aqueous solution of MP (set 1). The UV–Vis spectrum shows a peak at 295 nm, which is similar to literature values of pure MP [55]. After adding Au NPs into it (set 2), the peak is shifted to 313 nm (Spectrum of MP + Au NPs) and subsequently when a very small amount of NaOH is added to it, the peak further shifts to 400 nm (Spectrum of MP + Au NPs + base). It has been earlier reported and proved that peak of nitrophenols are observed at about 300–315 nm, whereas peak of nitrophenolate ion appears at around 400 nm [56]. In set 2 the peak at 313 nm indicates the formation of nitrophenol in acidic medium (in the absence of base) and the peak at 400 nm in the basic medium in set 3 shows the presence of nitrophenolate ion. Therefore, it can be easily seen that Au NPs are able to break the thiophosphate-ester bond of MP leading to the formation of nitrophenol and ultimately degrade MP.

The spectra obtained using MP + base is identical to the spectra obtained in set 3 (as shown below). This clearly shows that MP is degraded in presence of a base as we have already stated that it is a base catalysed reaction. This clearly proves that we can degrade MP without any externally added base in an acidic medium (pH in our case was around 5). Hence we can say that the glucan stabilized Au NPs are able to degrade MP without any other externally added agent. Moreover, on addition of base the peak shifts from 313 to 400 nm due to the formation of the nitrophenolate ion as the medium becomes basic in nature.

In order to further substantiate the above observation FTIR analysis of Au NPs-MP was carried out. Previous reports have shown that hydrolysis of methyl parathion (MP) in acidic medium gives two products, 4-nitrophenol and dimethylthiophosphoric acid [57]. After adding a small of NaOH solution, the colour of the solution turns bright yellow due to the formation of 4-nitrophenolate and sodium di-O-methyl thiophosphonate ions as evident from the peak around 400 nm obtained in UV–Vis spectra (set 3). From this observation it can be said that the formation of these ions from MP is a base catalyzed reaction. However, although our glucan capped Au NPs are unable to form the 4-nitrophenolate ions (as the medium is acidic in nature), they are able to break the phospho-ester bond and destroy the harmful effects of MP. To prove this contention we had studied the FT-IR spectrum

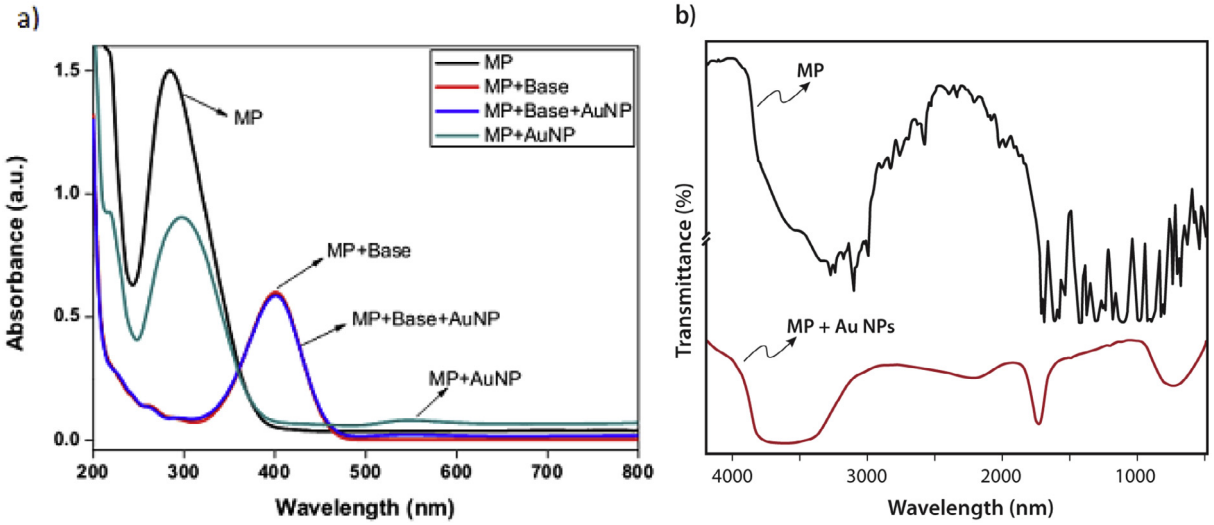

Fig. 5 (a) UV–Vis spectra of Methyl parathion solution, Methyl parathion solution along with glucan capped Au NPs solution and Methyl parathion and Au NPs solution with a small amount of base. (b) FT-IR spectroscopic measurement of Methyl parathion (MP) solution and Methyl parathion-Au NPs solution.

of MP and MP-Au NPs solutions (Fig. 5b). It was observed that in MP spectrum there was no sign of ─OH peak whereas in MP-Au NPs spectrum a broad peak of –OH was observed at about 3500 cm^{-1}. This clearly shows that the Au NPs were able to degrade MP as presumed above.

The proposed scheme for the above degradation is as follows. Hydrolysis of methyl parathion is carried out in NaOH by nucleophilic attack of hydroxyl ion to the phosphorus centre followed by concomitant cleavage of P─OAr bond (Scheme 1). But in acidic/neutral medium where no free hydroxyl ion is present, the phosphorus centre doesn't have enough electrophilicity to be attacked by the water molecule only, resulting in the cleavage of the P─OAr bond.

But in presence of Au NPs formed over there, even if the medium is at an acidic pH, as described in due course of the work, we believe that Au NPs possibly engage themselves to form some kind of covalent interaction with sulphur of '─P═S' moiety as can be expected from soft-soft (SHAB principle) interaction between Au NPs and Sulphur. This makes the phosphorus centre of MP more electrophilic in nature which in turn allows water molecule, present in acidic pH medium, to attack and thus became capable to cleave the 'P─OAr' bond (Scheme 1).

3.4. Effect of Au NPs on Rhodamine B fluorescence in different solvents

Rhodamine B, a common fluorophore and a suspected carcinogenic compound containing a warning on its product label can be easily detected using a fluorimeter. As Au NPs are capable of quenching the fluorescence intensity of any fluorescent probe, the glucan capped Au NPs were mixed with Rhodamine B. Fig. 6 depicts the fluorescence emission spectra of Rhodamine B (Rh B) (2×10^{-4} M, λ_{ex} = 360 nm) solution with different concentrations of Au NPs at 25 °C in four different solvents. The maximum emission wavelength for Rh B in water was observed at about 578 nm. The same trends were observed for the other three solvents viz., ethanol, isopropanol and ethylene glycol. With increase in concentration of glucan capped Au NPs (Fig. 6a), the fluorescence intensity of Rh B

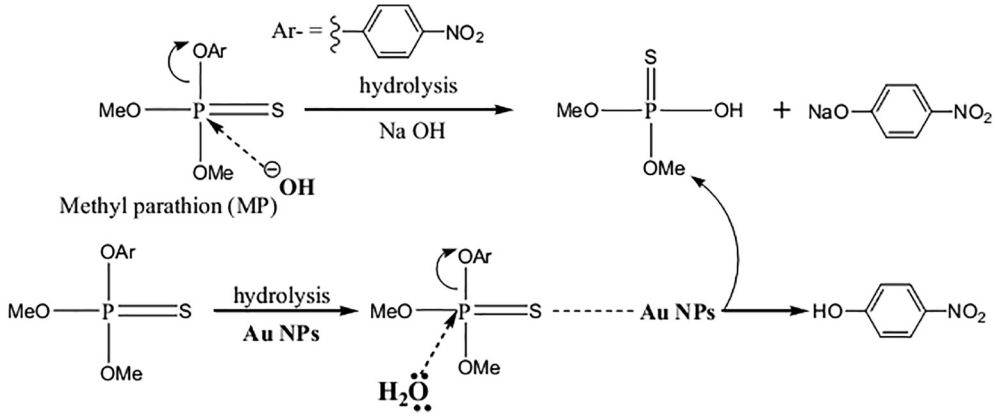

Scheme 1 Plausible mechanism of degradation of Methyl Parathion by glucan capped Au NPs.

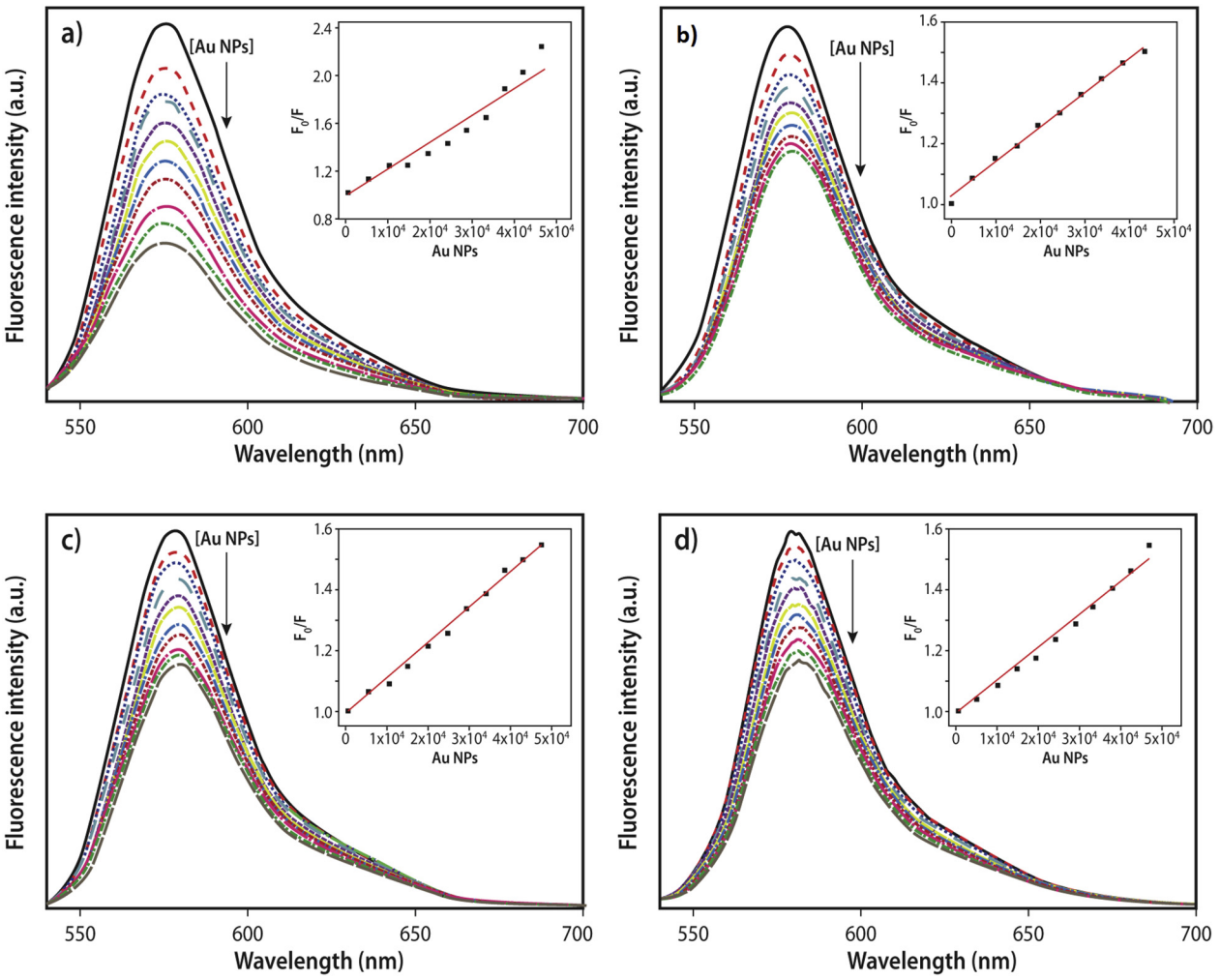

Fig. 6 Rhodamin B fluorescence quenching by Au NPs in three different solvents of increasing viscosity (a) Water, (b) Ethanol, (c) Isopropanol and (d) Ethylene glycol. Corresponding Stern-Volmer plots shown in inset.

in water decreased progressively, however, the emission wavelength at maximum emission was almost constant. From this observation one can conclude that there was no observable photochemical reaction between Au NPs and the dye in water medium. This clearly shows that the Au NPs sense and quench the fluorescence intensity of Rh B resulting in a decrease in the dye concentration in the mixture. This nature of the curve indicates that the Au NPs can be used as an effective tool in minimizing the carcinogenic effect of the dye. Similar behaviour was observed for Rh B with increasing concentrations of Au NPs in the three other solvents of different viscosities (Fig. 6b, c and d). Now, the Rh B fluorescence quenching mechanism was analyzed following the standard Stern-Volmer equation: [58]

$$F_0/F = 1 + K_{sv}[Q] \quad (1)$$

$$K_{sv} \propto 1/\eta \quad (2)$$

where F_0 and F are the fluorescence intensities in the absence and presence of quencher, respectively. K_{sv} and [Q] are the Stern–Volmer quenching constant and quencher i.e., Au NPs concentration here, respectively. Fluorescence quenching occurs via two types of mechanisms, dynamic and static. For dynamic quenching mechanism, the quenching rate constant increases with increasing temperature [59] and the Stern-Volmer constant (K_{sv}) decreases with increasing viscosity (η) (Eq. (2)). Stern-Volmer plots of Rh B-Au NPs system in four different solvents of different viscosities were shown in Fig. 6a, b, c and d. Within experimental limits, all the plots obtained were linear and showed a correlation coefficient of above 0.98. From the slopes of the linear plots, the Stern-Volmer quenching constants (K_{sv}) were calculated and listed in Table 1. Table 1 clearly indicates that the probable quenching process of Rh B interacting with Au NPs were dynamic rather than static in nature, because all the Stern-Volmer plots

Table 1 Change in Stern-Volmer constant with change in solvent viscosity.

Solvent	Viscosity (cP) at 25 °C	K_{sv}	Intercept
Water	0.890	2269	1.00
Ethanol	1.095	1169	1.02
Isopropanol	1.960	1146	1.00
Ethylene glycol	16.10	1080	0.989

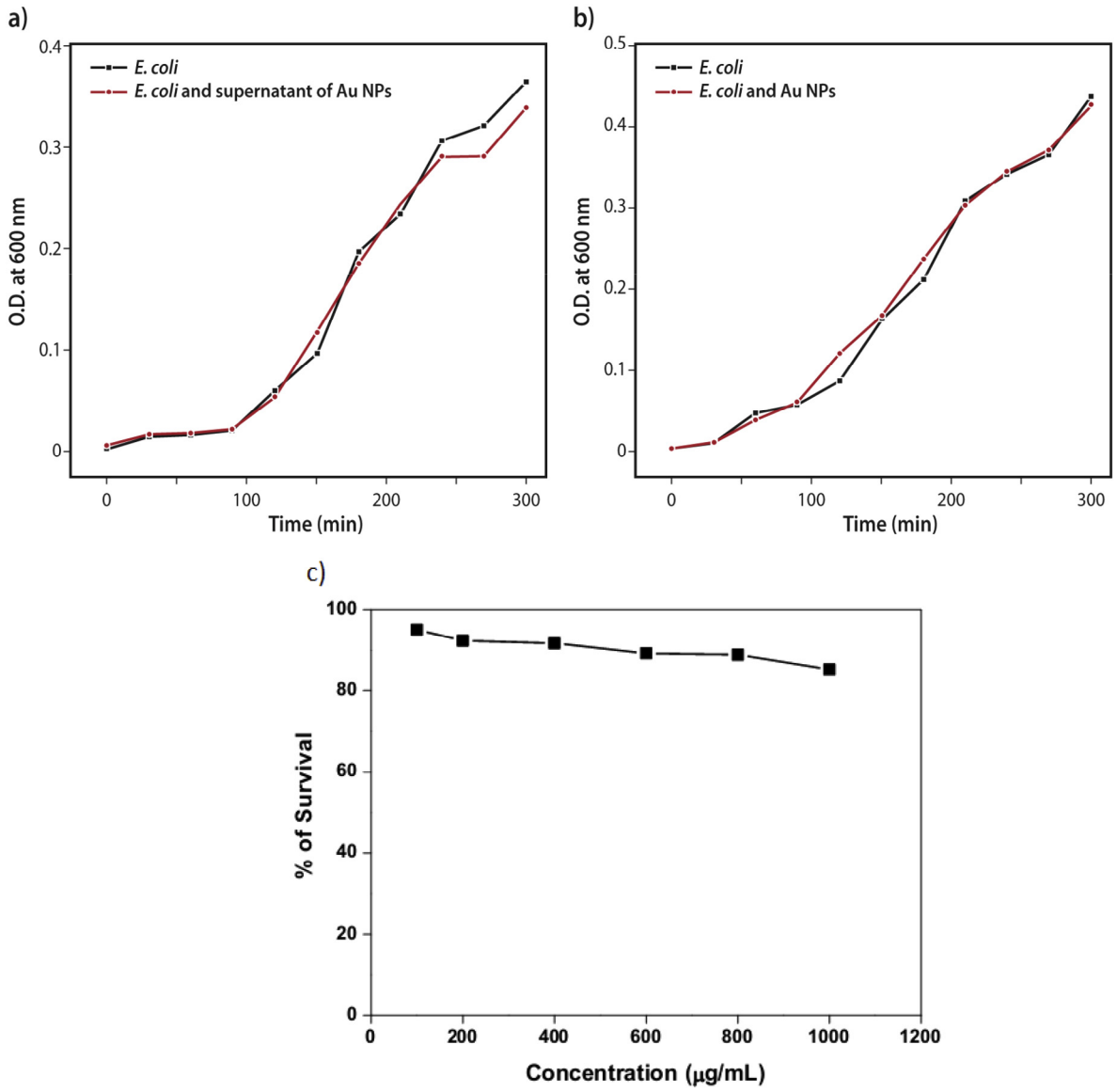

Fig. 7 Toxicity study using optical method. (a) Comparison of O.D. at 600 nm between *E. coli* strain and the supernatant of Au NPs sol after centrifugation (b) Comparison of O.D. at 600 nm between *E. coli* strain and the Au NPs sol (c) MTT assay of L929 cell with glucan capped Au NPs.

were linear and the observed K_{sv} decreased with increasing viscosity, which is expected for dynamic quenching.

3.5. Analysis of antimicrobial and antitoxicity properties of Au NPs

β-D-glucan stabilized Au NPs and its supernatant did not show any antimicrobial activity when studied with Gram positive bacteria *Staphylococcus aureus* and Gram negative bacteria *Klebsiella aerogenes* and *Escherichia coli* using the standard cup plate method. The Au NP did not exhibit any zone of inhibition which may be probably due to no reasonable interaction of the β-D-glucan stabilized Au NP with the bacterial cell wall and hence these Au NPs did not have any antimicrobial activity.

Nanoparticles targeted for clinical purposes must be reasonably non toxic and hence toxicity of different nanomaterials has been a subject of great interest. Earlier reports have shown that gold, known to be safe and chemically inert in the nano-scale can be used in photothermal therapy and as imaging agents in living system [8]. Since, the β-D-glucan stabilized Au NPs exhibits absence of antimicrobial activity, the toxicity studies were carried out on the growth of Gram negative Escherichia coli (*E. coli*) bacteria cells. Fig. 7 depicts the growth curve of *E. coli* cells and *E. coli* with Au NPs supernatant from the data of absorbance against time. The supernatant had no effect on the growth of E. coli cells as evident from Fig. 7a. Cells grown in presence of β-D-glucan stabilized Au NPs also exhibited similar results which indicate that the β-D-glucan stabilized Au NPs had no effect on the growth of the bacterial cells.

The non toxic nature of the glucan stabilized nanoparticles is also confirmed when the gold nanoparticles did not exhibit any cytotoxicity on Mouse fibroblast L929 (as shown in the Fig. 7c) as the nanoparticles had no effect on normal cell growth and viability as evident from proliferative assay of normal cell line (L929) in the concentration range (100–1000 μg/mL). Thus we can say that the β-D-glucan stabilized Au NPs did not affect normal cell growth and can have possible medicinal applications, similar to our other systems and observations of earlier researchers [60,47].

4. Conclusions

β-D-Glucan, a natural carbohydrate polymer capped gold nanoparticles (Au NPs) were synthesized in a green way and characterized using different tools. The Au NPs exhibited multipod like structure and were crystalline in nature. β-D-Glucans extracted from naturally occurring edible mushrooms have application in different medicinal areas and keeping this idea in mind we tried to study the effect of β-D-Glucan stabilized Au NPs on the environment. The Au NPs were able to sense and degrade harmful pesticide like methyl parathion, a common pesticide extensively used in India. These Au NPs can also be used to sense the presence of a common fluorescent dye like Rhodamine B, which exhibit carcinogenic property. The Au-NPs quench the fluorescence of Rhodamine B, thus minimizing its negative effect. The above quenching was dynamic in nature obeying Stern Volmer plot. The Au NPs are also safe as evident from the preliminary studies having potential medicinal application.

Acknowledgements

We gratefully acknowledge the financial support for this work by DST, India through INSPIRE fellowship. Financial support of DST-FIST, India for instrumental grant is gratefully acknowledged. We convey our gratitude to CRNN, Kolkata for various types of instrumental facilities availed by us.

References

[1] Y.W. Cao, R. Jin, C.A. Mirkin, DNA-modified core–shell Ag/Au nanoparticles, J. Am. Chem. Soc. 123 (2001) 7961–7962.
[2] R.C. Hayward, D.A. Saville, I.A. Aksay, Electrophoretic assembly of colloidal crystals with optically tunable micropatterns, Nature 404 (2000) 56–59.
[3] N. Pradhan, A. Pal, T. Pal, Catalytic reduction of aromatic nitro compounds by coinage metal nanoparticles, Langmuir 17 (2001) 1800–1802.
[4] N. Pradhan, A. Pal, T. Pal, Silver nanoparticles catalyzed reduction of aromatic nitro compounds, Colloids Surf. A Physiochem. Eng. Aspects 196 (2002) 247–257.
[5] F. Zeng, C. Hou, S.Z. Wu, X.X. Liu, Z. Tong, S.N. Yu, Silver nanoparticles directly formed on natural macroporous matrix and their anti-microbial activities, Nanotechnology 18 (2007) 8, 055605.
[6] Y. Junejo, A. Baykal, Sirajuddin, Green chemical synthesis of silver nanoparticles and its catalytic activity, J. Inorg. Organomet. Polym. Mater. 24 (2014) 401–406.
[7] K.B.A. Ahmed, S. Subramanian, A. Sivasubramanian, G. Veerappan, A. Veerappan, Preparation of gold nanoparticles using Salicornia brachiata plant extract and evaluation of catalytic and antibacterial activity, Spectrochim. Acta Mol. Biomol. Spectrosc. 130 (2014) 54–58.
[8] P.K. Jain, X. Huang, I.H. El-Sayed, M.A. El-Sayed, Noble metals on the nanoscale: optical and photothermal properties and some applications in imaging, sensing, biology, and medicine, Acc. Chem. Res. 41 (2008) 1578–1586.
[9] K.L. Kelly, E. Coronado, L.L. Zhao, G.C. Schatz, The optical properties of metal nanoparticles: the influence of size, shape, and dielectric environment, J. Phys. Chem. B 107 (2003) 668–677.
[10] K. Bankura, D. Rana, M.M.R. Mollick, S. Pattanayak, B. Bhowmick, N.R. Saha, I. Roy, T. Midya, G. Barman, D. Chattopadhyay, Dextrin mediated synthesis of AgNPs for colorimetric assays of Cu^{2+} ion and AuNPs for catalytic activity, Int. J. Biol. Macromolec. 80 (2015) 309–316.
[11] M.M.R. Mollick, D. Rana, S.K. Dash, S. Chattopadhyay, B. Bhowmick, D. Maity, D. Mondal, S. Pattanayak, S. Roy, M. Chakraborty, D. Chattopadhyay, Studies on green synthesized silver nanoparticles using *Abelmoschus esculentus* (L.) pulp extract having anticancer (in vitro) and antimicrobial applications, Arabian J. Chem. (2015), org/10.1016/j.arabjc.2015.04.033.
[12] D. Maity, S. Pattanayak, M.M.R. Mollick, D. Rana, D. Mondal, B. Bhowmick, S.K. Dash, S. Chattopadhyay, B. Das, S. Roy, M. Chakraborty, D. Chattopadhyay, Green one step morphosynthesis of silver nanoparticles and their antibacterial and anticancerous activities, New J. Chem. 40 (2016) 2749–2762.
[13] L. Dykman, N. Khlebtsov, Gold nanoparticles in biomedical applications: recent advances and perspectives, Chem. Soc. Rev. 41 (2012) 2256–2282.
[14] I. Pastoriza-Santos, L.M. Liz-Marzan, Formation and stabilization of silver nanoparticles through reduction by N,N-dimethylformamide, Langmuir 15 (1999) 948–951.
[15] L. Rivas, S. Sanchez-Cortes, J.V. Garcia-Ramos, G. Morcillo, Growth of silver colloidal particles obtained by citrate reduction to increase the Raman enhancement factor, Langmuir 17 (2001) 574–577.
[16] A.K. Singh, O.N. Srivastava, One-step green synthesis of gold nanoparticles using black cardamom and effect of pH on its synthesis, Nanoscale Res. Lett. 10 (2015) 353–365.
[17] M. Nasrollahzadeh, M. Atarod, B. Jaleh, M. Gandomirouzbahani, n situ green synthesis of Ag nanoparticles on graphene oxide/TiO_2 nanocomposite and their catalytic activity for the reduction of 4-nitrophenol, congo red and methylene blue, Ceram. Int. 42 (2016) 8587–8596.
[18] K. Esumi, N. Takei, T.Y. Oshimura, Antioxidant-potentiality of gold–chitosan nanocomposites, Colloids Surf. B 32 (2003) 117–123.
[19] R.C. Mucic, J.J. Storhoff, C.A. Mirkin, R.L. Letsinger, DNA-directed synthesis of binary nanoparticle network materials, J. Am. Chem. Soc. 120 (1998) 12674–12675.
[20] C.L. Chen, P. Zhang, N.L. Rosi, A new peptide-based method for the design and synthesis of nanoparticle superstructures: construction of highly ordered gold nanoparticle double helices, J. Am. Chem. Soc. 130 (2008) 13555–13557.
[21] J.M. Slocik, M.O. Stone, R.R. Naik, Synthesis of gold nanoparticles using multifunctional peptides, Small 1 (2005) 1048–1052.
[22] M.M.R. Mollick, B. Bhowmick, D. Maity, D. Mondal, M.K. Bain, K. Bankura, J. Sarkar, D. Rana, K. Acharya, D. Chattopadhyay, Green synthesis of silver nanoparticles using Paederia foetida L. leaf extract and assessment of their antimicrobial activities, Int. J. Green Nanotechnol. 4 (2012) 230–239.
[23] S. Pattanayak, M.M.R. Mollick, D. Maity, S. Chakraborty, S. K. Dash, S. Chattopadhyay, S. Roy, D. Chattopadhyay, M. Chakraborty, *Butea monosperma* bark extract mediated green

synthesis of silver nanoparticles: characterization and biomedical applications, J. Saudi Chem. Soc. 21 (2017) 673–684.
[24] Z. Gao, R. Su, R. Huang, W. Qi, Z. He, Glucomannan-mediated facile synthesis of gold nanoparticles for catalytic reduction of 4-nitrophenol, Nanoscale Res. Lett. 9 (2014) 404–411.
[25] P. Raveendran, J. Fu, S.L. Wallen, Completely "Green" synthesis and stabilization of metal nanoparticles, J. Am. Chem. Soc. 125 (2003) 13940–13941.
[26] P. Mukherjee, A. Ahmad, D. Mandal, S. Senapati, S.R. Sankar, M.I. Khan, R. Ramani, R. Parischa, P.V. Ajayakumar, M. Alam, M. Sastry, R. Kumar, Bioreduction of $AuCl^{4-}$ ions by the fungus, Verticillium sp. and surface trapping of the gold nanoparticles formed, Angew. Chem. Int. Ed. 40 (2001) 3585–3588.
[27] D. Philip, Biosynthesis of Au, Ag and Au–Ag nanoparticles using edible mushroom extract, Spectrochim. Acta Mol. Biomol. Spectrosc. 73 (2009) 374–381.
[28] T. Gardiner, Beta–glucan biological activities: a review, GlycoScience. 1 (2000) 1–6.
[29] T. Gardiner, G. Carter, Beta-glucan biological activities: a review (condensed version), GlycoScience 1 (2000) 1–2.
[30] B.A. Stone, A.E. Clarke, Chemistry and Biology of 1,3-β-Glucans, Melbourne, La Trobe University Press, Australia, 1992.
[31] A. Chatterjee, S. Khatua, S. Chatterjee, S. Mukherjee, A. Mukherjee, S. Paloi, K. Acharya, S.K. Bandyopadhyay, Polysaccharide-rich fraction of Termitomyces eurhizus accelerate healing of indomethacin induced gastric ulcer in mice, Glycoconjugate J. 30 (2013) 759–768.
[32] A. Chatterjee, K. Acharya, Include mushroom in daily diet—A strategy for better hepatic health, Food Rev. Int. 32 (2016) 68–97.
[33] M.E. Valverde, T. Hernández-Pérez, O. Paredes-López, Edible mushrooms: improving human health and promoting quality life, Int. J. Microbiol. (2015) 14, https://doi.org/10.1155/2015/37638. Article ID 376387.
[34] D.L. Williams, R.B. McNamee, E.L. Jones, H.A. Pretus, H.E. Ensley, I.W. Browder, N.R. Di Luzio, A method for the solubilization of a (1→3)-α-D-glucan isolated from Saccharomyces cerevisiae, Carbohydr. Res. 219 (1991) 203–213.
[35] D.L. Williams, H.A. Pretus, R.B. McNamee, E.L. Jones, H.E. Ensley, I.W. Browder, Development of a water-soluble sulfated (1→3)-α-D-glucan biological response modifier derived from Saccharomyces cerevisiae, Carbohydr. Res. 235 (1992) 247–257.
[36] S.T. Chang, W.A. Hayes, The Biology and Cultivation of Edible Mushrooms, Academic Press, New York, NY, 1978.
[37] M.D. Mehrotra, Mycorrhiza of Indian Forest Trees, Indian Council of Forestry Research and Education, Special ed., New Forest, Dehradun, India, 1991, pp. 1–294.
[38] P. Pradhan, S. Banerjee, A. Roy, K. Acharya, Role of wild edible mushrooms in the Santal livelihood in lateritic region of West Bengal, J. Bot. Soc. Bengal. 64 (2010) 61–65.
[39] N. Teaumroong, W. Sattayapisut, T. Teekachunhatean, N. Boonkerd, Using agricultural wastes for Tricholoma crassum (Berk.) Sacc. production, Springer, Heidelberg, Germany, 2002, pp. 231–236.
[40] M. Tantiyaporn, A. Ritthiboon, Mating system and genetic variations of Tricholoma crassum (Berk.) Sacc. in some area of Thailand by isozyme electrophoresis and PCR-RFLP method, Int. J. Med. Mushrooms 7 (2005) 475.
[41] S. Ray, S. Sarkar, S. Kundu, Extracellular biosynthesis of silver nanoparticles using the mycorrhizal mushroom Tricholoma crassum (berk.) Sacc: its antimicrobial activity against pathogenic bacteria and fungus, including multidrug resistant plant and human bacteria, Dig. J. Nanomater. Biostruct. 6 (2011) 1289–1299.
[42] J.H. Hong, B. Manochai, G. Trakoontivakorn, V.N. Thalang, Fibrinolytic activity of Thai indigenous vegetables, Kasetsart J. (Nat. Sci.) 38 (2004) 241–246.
[43] P. Patra, S.K. Bhanja, I.K. Sen, A.K. Nandi, S. Samanta, D. Das, K.S.P. Devi, T.K. Maiti, K. Acharya, S.S. Islam, Structural and immunological studies of hetero polysaccharide isolated from the alkaline extract of Tricholoma crassum (Berk.) Sacc, Carbohydr. Res. 362 (2012) 1–7.
[44] S. Samanta, K. Maity, A.K. Nandi, I.K. Sen, K.S.P. Devi, S. Mukherjee, T.K. Maiti, K. Acharya, S.S. Islam, A glucan from an ectomycorrhizal edible mushroom Tricholoma crassum (Berk.) Sacc: isolation, characterization, and biological studies, Carbohydr. Res. 367 (2013) 33–40.
[45] K.A. Kang, J. Wang, J.B. Jasinski, S. Achilefu, Fluorescence manipulation by gold nanoparticles: from complete quenching to extensive enhancement, J. Nanobiotechnol. 9 (2011) 16–29.
[46] G.R. Bardajee, Z. Hooshyar, M. Khanjari, Dye fluorescence quenching by newly synthesized silver nanoparticles, J. Photochem. Photobiol. A 276 (2014) 113–121.
[47] S. Pattanayak, S. Chakraborty, M.M.R. Mollick, I. Roy, S. Basu, D. Rana, S.S. Gauri, D. Chattopadhyay, M. Chakraborty, *In situ* fluorescence of lac dye stabilized gold nanoparticles; DNA binding assay and toxicity study, New J. Chem. 40 (2016) 7121–7131.
[48] S. Saha, S. Khatua, S. Paloi, K. Acharya, Antioxidant and nitric oxide synthase activation properties of water soluble polysaccharides from *Pleurotus florida*, Int. J. Green. Pharm. 7 (2013) 182–188.
[49] K. Das, A. Uppal, R.K. Saini, G.K. Varshney, P. Mondal, P.K. Gupta, Hyper-Rayleigh scattering from gold nanoparticles: effect of size and shape, Spectrochim. Acta Mol. Biomol. Spectrosc. 128 (2014) 398–402.
[50] A. Villares, L. Mateo-Vivaracho, E. Guillamón, Structural features and healthy properties of polysaccharides occurring in mushrooms, Agriculture 2 (2012) 452–471.
[51] S. Li, Y. Shen, A. Xie, X. Yu, X. Zhang, L. Yang, C. Li, Rapid, room-temperature synthesis of amorphous selenium/protein composites using *Capsicum annuum* L. extract, Nanotechnology 18 (2007) 405101–405110.
[52] Y. Shi, X. Sun, Spectrum and Chemical Identification of Organic Compounds, Nanjing, Jiangsu Science Technology Press, China, 1988.
[53] C. Sun, R. Qu, H. Chen, C. Ji, C. Wang, Y. Sun, B. Wang, Degradation behaviour of chitosan chains in the 'green' synthesis of gold nanoparticles, Carbohydr. Res. 343 (2008) 2595–2599.
[54] I.K. Sen, K. Maity, S.S. Islam, Green synthesis of gold nanoparticles using a glucan of an edible mushroom and study of catalytic activity, Carbohydr. Polym. 91 (2013) 518–528.
[55] A.M. Mensah-Brown, Analysis of the Detection of Organophosphate Pesticides in Aqueous Solutions Using Polymer Coated SH-SAW Devices Ph.D. Dissertations, Marquette University, Milwaukee, WI, 2010.
[56] A.I. Biggs, A spectrophotometric determination of the dissociation constants of p-nitrophenol and papaverine, Trans. Faraday Soc. 50 (1954) 800–802.
[57] S.B. Pakala, P. Gorla, A.B. Pinjari, R.K. Krovidi, R. Baru, M. Yanamandra, M.J. Merrick, D. Siddavattam, Biodegradation of methyl parathion and p-nitrophenol: evidence for the presence of a p-nitrophenol 2-hydroxylase in a Gram-negative Serratia sp. strain DS001, Appl. Microbiol. Biotechnol. 73 (2007) 1452–1462.
[58] D. Forcha, K.J. Brown, Z. Assefa, Spectrochim. Luminescence absorption, and Stern-Volmer studies of cerium chloride and nitrate compounds in acidic and neutral aqueous, and non-aqueous solutions, Acta Mol. Biomol Spectrosc. 103 (2013) 90–95.

[59] A.S. Al-Kady, M. Gaber, M.M. Hussein, E.M. Ebeid, Structural and fluorescence quenching characterization of hematite nanoparticles, Spectrochim. Acta Mol. Biomol. Spectrosc. 83 (2011) 398–405.

[60] A.M. Alkilany, C.J. Murphy, Toxicity and cellular uptake of gold nanoparticles: what we have learned so far?, J Nanopart. Res. 12 (2010) 2313–2333.